Electronic Supplementary Information (ESI) for:

Recognizing the Reactive Sites of $SnFe_2O_4$ for the Oxygen Evolution Reaction: Synergistic Effect of Sn^{II} and Fe^{III} in Stabilizing Reaction Intermediates

Anubha Rajput[†], Pandiyan Sivasakthi[§], Pralok K. Samanta[§*], and Biswarup Chakraborty[†*]

[†]Department of Chemistry, Indian Institute of Technology Delhi, Hauz Khas, 110016, New Delhi, India

[§]Department of Chemistry, Birla Institute of Technology and Science Pilani (BITS Pilani), Hyderabad Campus, Hyderabad-500078, India

***E-mail:** pralokkumar.samanta@hyderabad.bits-pilani.ac.in

cbiswarup@chemistry.iitd.ac.in

Table of Contents

Experimental Section

Preparation and deposition of catalyst ink on the electrode surface. Three-dimensional and porous network like nickel foam (NF) of thickness ca. 0.5 mm were chosen as electrode substrates for catalyst deposition. The following steps were sequentially employed to prepare a catalyst ink and subsequently to deposit it on NF: (i) The sheet of NF was cut into several pieces of dimension 1x2 cm^2. It was then washed ultrasonically in 0.1 N HCl followed by washing twice with milli-Q water and once with acetone. The electrodes were then dried at 50°C overnight in an oven. (ii) To prepare the ink, Nafion was used as a medium to disperse the catalyst in an aqueous medium. Nafion is a conductive, sulfonated tetrafluoroethylene-based fluoropolymer which binds the catalyst particles on the electrode surface. Nafion was diluted to 1.0 wt% in ethanol, and 50 mg $SnFe_2O_4$ was added to it. The mixture was homogenized by sonicating it for 10 minutes at room temperature. (iii) The prepared ink was drawn in a pipette and was deposited dropwise on a pre-cleaned NF surface. The 1x1 cm^2 surface area was covered with the ink after which the electrode was left to dry at room temperature overnight.

Characterization and Analysis Methods

1.1. Powder X-ray diffraction (PXRD)

The phase purity and crystalline structure of $SnFe_2O_4$ and Fe_3O_4 were characterized by powder X-ray diffraction on Bruker D8 Advance X-ray diffractometer equipped with Cu Kα ($K\alpha_1$ = 1.540598 Å, $K\alpha_2$ = 1.544426 Å, Kα ratio 0.5, $K\alpha_{av}$ = 1.541874 Å) X-ray tubes. The diffraction pattern was recorded in the 2θ range of 10° to 80°. The obtained diffractogram was matched with the respective JCPDS (Joint Committee on Powder Diffraction Standards) data file of the compound to establish the phase purity. To calculate the crystallite size of the nano-particle, Scherrer's formula was used.[1]

$$Crystallite\ size(D) = \frac{K\lambda}{\beta cos\theta}$$

where θ is the angle between the incident and reflected X-rays, β is the full width at half maxima, λ is the X-ray wavelength = 1.5406 Å (Cu Kα), and K is the shape factor constant = 0.89.

1.2. Raman spectroscopy.

Raman spectroscopy of all the material was recorded with HORIBA EVOLUTION, HORIBA Jobinyvon, France, equipped with a 532 nm laser. All the samples were set at 50X and crystalline Si was used for calibration. Raman spectra were recorded with the materials by placing them on the Al foil, and before each spectral recording, the instrument was calibrated with the Si wafer.

1.3. Computational details

The Vienna Ab initio Simulation Program (VASP) was used to perform all periodic density functional theory (DFT) calculations.[2] The calculations were performed using a plane-wave basis with a plane-wave energy cutoff value of 500 eV. The pseudopotentials were used to describe the ion-electron correlations followed the projector-augmented wave (PAW) approach. Additionally, the exchange-correlation function was treated with the Perdew-Burke-Ernzerhof (PBE) functional within the generalized gradient approximation (GGA).[3, 4] The van der Waals (vdW) interactions between the $SnFe_2O_4$ layer and OER organic molecules were accurately predicted by applying the DFT-D3 correction. The Monkhorst-Pack scheme with a 2 × 2 × 1 grid was employed for Brillouin zone integration.[5] All structures were fully relaxed using the conjugate gradient method until the threshold energy of 1×10^{-6} eV was reached. During geometry relaxation, the $SnFe_2O_4$ layers below the second layer were fixed, while the layers above were relaxed to interact freely with the OER reaction. All atoms in the complex systems were allowed to move freely along the X, Y, and Z directions. To avoid lateral interaction between the next periodic image, more than 15 Å vacuum region was maintained along the Z-direction. To avoid lateral interaction between the next periodic image, more than 15 Å vacuum region was maintained along the Z-direction. Similar OER mechanisms are reported in literature.[6, 7]

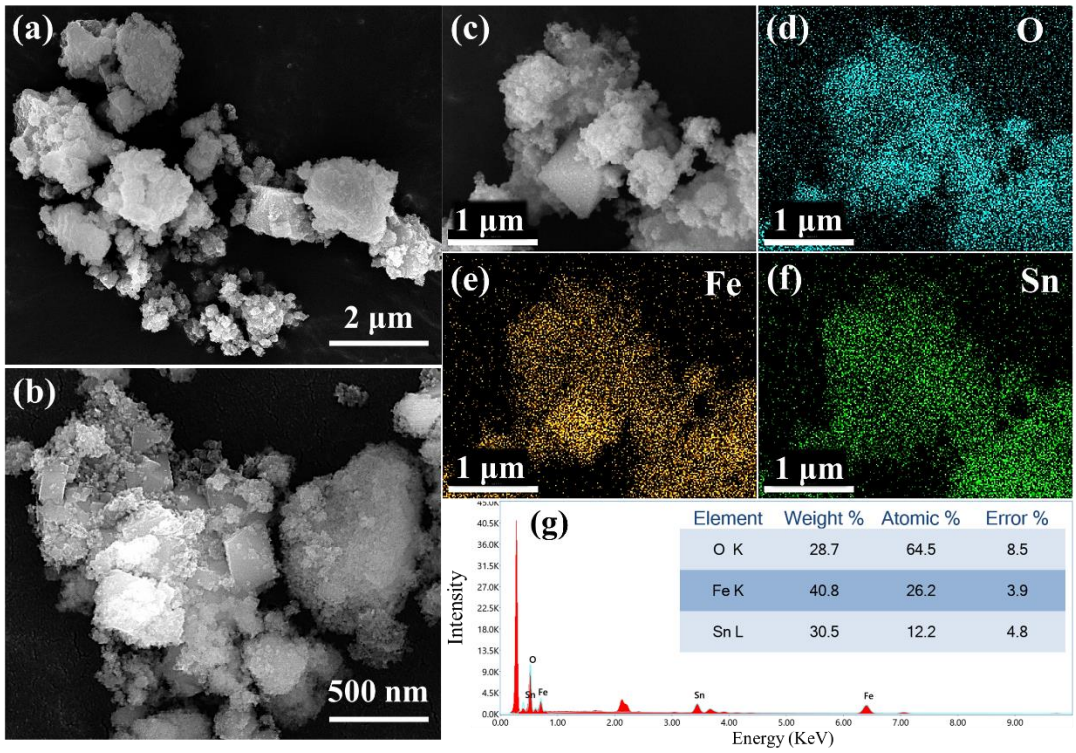

Figure S1. Microscopic FESEM characterization of as prepared $SnFe_2O_4$/NF (a-b) The high resolution image showing the aggregated grain-like morphology of the $SnFe_2O_4$ particles. SEM-EDX elemental mapping showing the homogeneous distribution of (d) O, (e) Fe, (f) Sn (g) The EDX mapping showing the relative ratio of elements present on the surface.

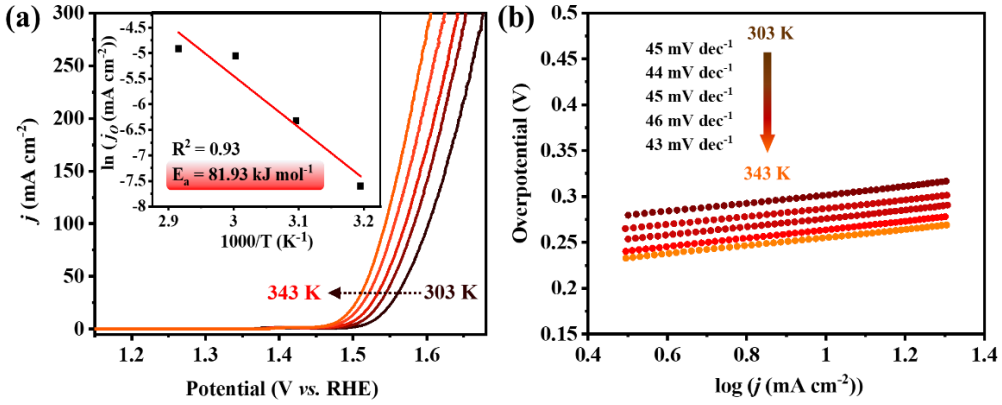

Figure S2. (a) Temperature-dependent OER in 1 M KOH (scan rate 1 mV s^{-1}) catalyzed by Fe_3O_4. Inset shows a ln(j_0) vs 1000/T plot to determination of the corresponding activation energy of the reaction (b) Tafel slope values for Fe_3O_4 in 1 M KOH over the temperature range of 303-343 K.

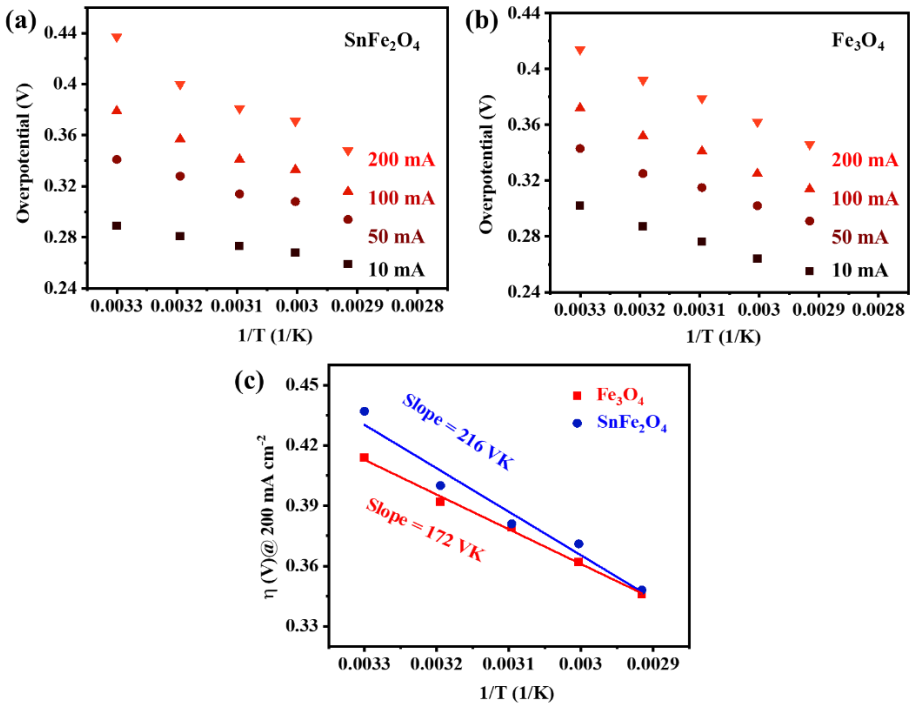

Figure S3. A plot between η vs. 1/T at different higher current densities of 10, 50, 100, and 200 mA cm^{-2} for (a) $SnFe_2O_4$ and (b) Fe_3O_4. (c) Plot between η vs. 1/T at high current density showing a higher dependence of overpotential on temperature in case of $SnFe_2O_4$.

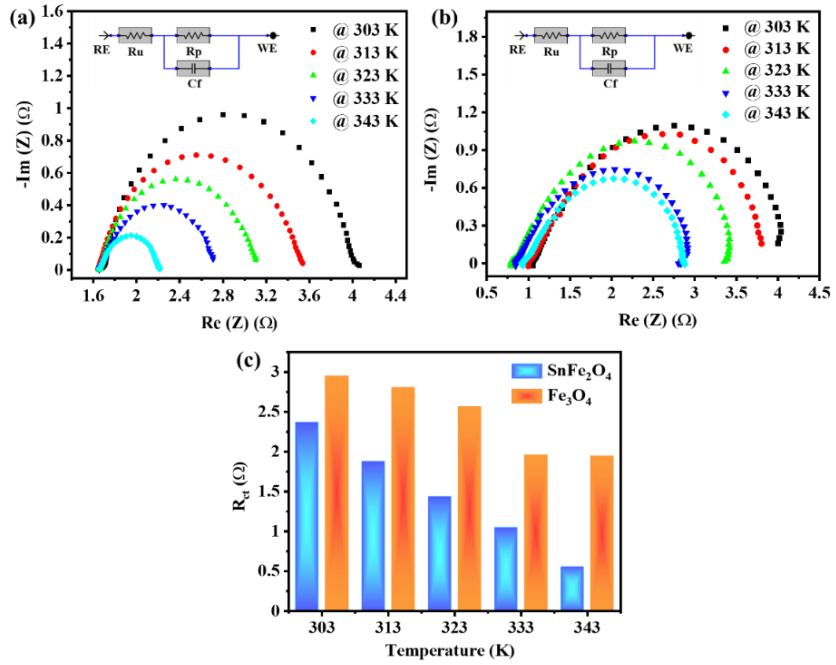

Figure S4. Temperature-dependent impedance study of (a) $SnFe_2O_4$ and (b) Fe_3O_4. (c) Bar chart showing a comparative effect of temperature on the charge transfer resistance (R_{ct}) of $SnFe_2O_4$ and Fe_3O_4.

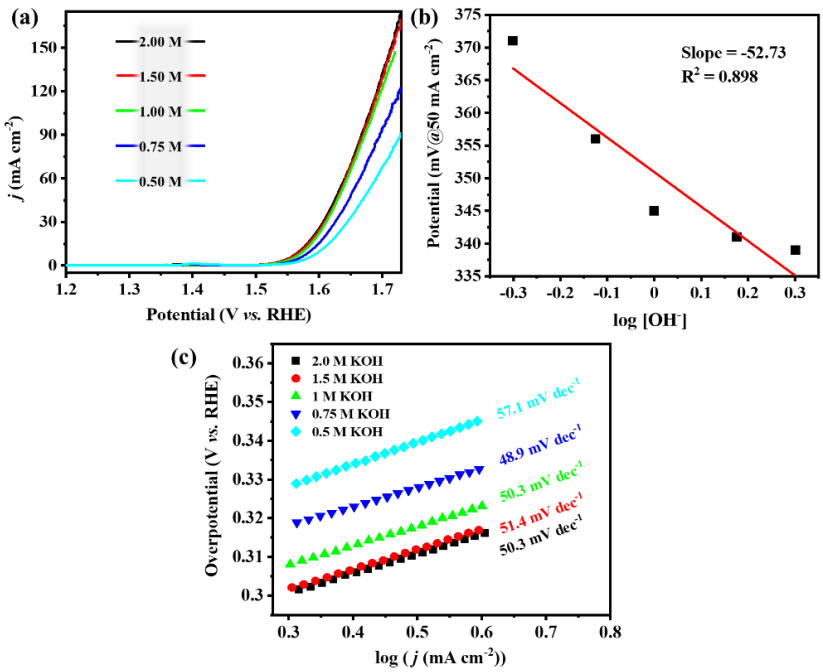

Figure S5. (a) Polarization curves obtained at the variable concentrations of the electrolyte from 0.5 to 2 M KOH (scan rate 1 mV s^{-1}) for Fe_3O_4. (b) Plot of the overpotential vs logarithmic of hydroxide concentration at a constant current. The slope of the linear fit divided by the Tafel slope gives the

reaction order (m). (c) Corresponding Tafel slope at the variable concentrations of the electrolyte from 0.5 to 2 M KOH.

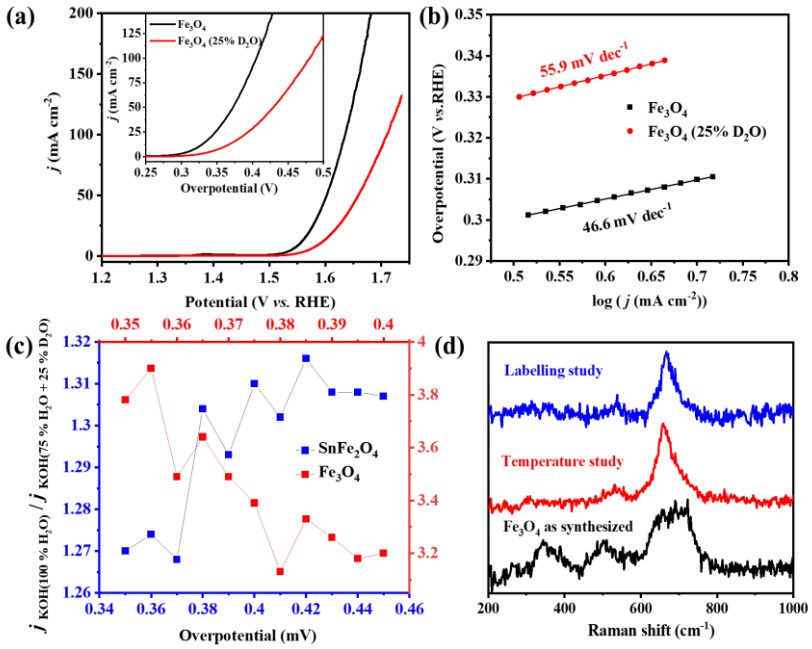

Figure S6. (a) Polarization curves for Fe_3O_4 in presence of 1 M KOH in H_2O and 1 M KOH in 25% D_2O. (b) Tafel slopes for Fe_3O_4 in presence of 1 M KOH in H_2O and 1 M KOH in 25% D_2O. (c) KIE for $SnFe_2O_4$ and Fe_3O_4 (d) Comparative Raman spectroscopic study of as prepared Fe_3O_4, after the temperature-variation study, and after the KIE study.

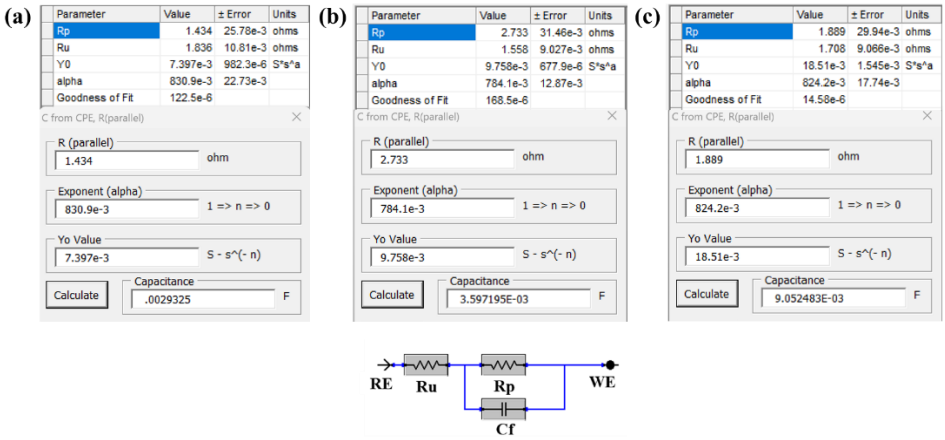

Figure S7. The C_{dl} values obtained from the CPE fitting of the Nyquist plot for $SnFe_2O_4$ in (a) LiOH, (b) NaOH, and (c) KOH.

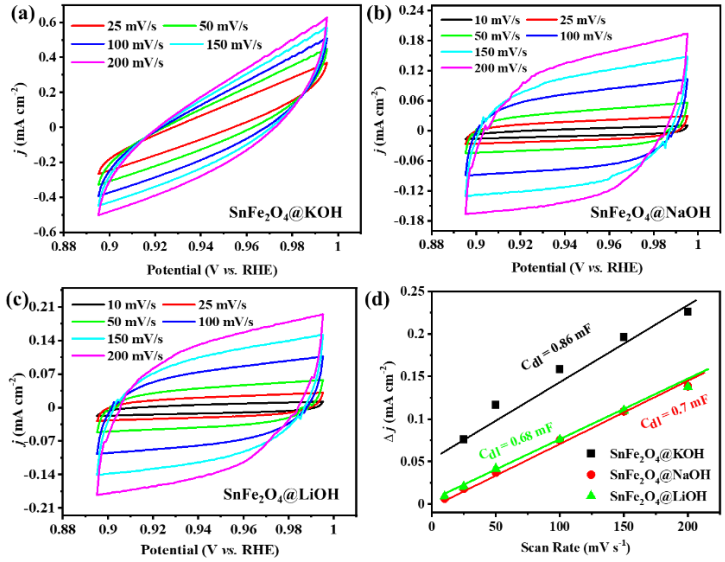

Figure S8. Cyclic voltammetry (CV) in non-faradic region performed with $SnFe_2O_4$/NF at different scan rates (10, 25, 50, 100, 150, and 200 mV s^{-1}) in (a) 1 M KOH, (b) 1 M NaOH, and (c) 1 M LiOH to determine the double layer capacitance (C_{dl}). (d) The plot of Δj vs. scan rate from the CV curves. The linear fitting is used to determine the C_{dl} values in corresponding electrolytes.

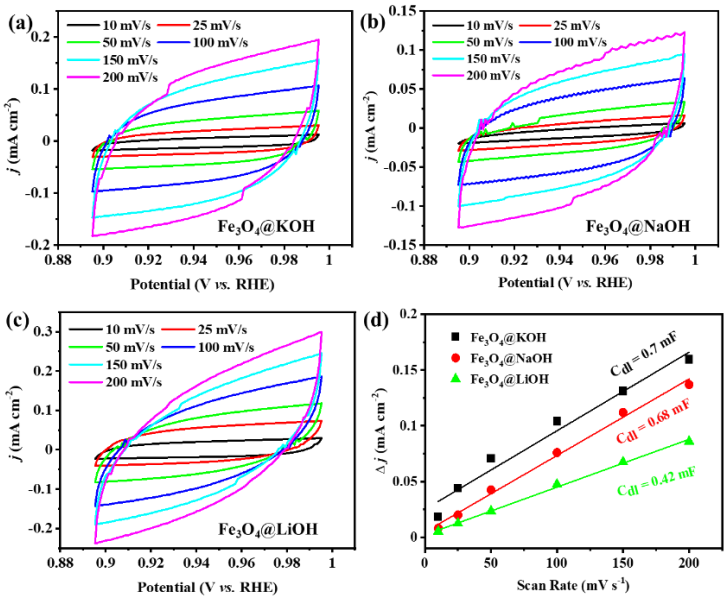

Figure S9. The CV in non-faradic region performed with Fe_3O_4/NF at different scan rates (10, 25, 50, 100, 150, and 200 mV s^{-1}) in (a) 1 M KOH, (b) 1 M NaOH, and (c) 1 M LiOH (d) The plot of Δj vs. scan rate to determine the C_{dl} in different electrolytes.

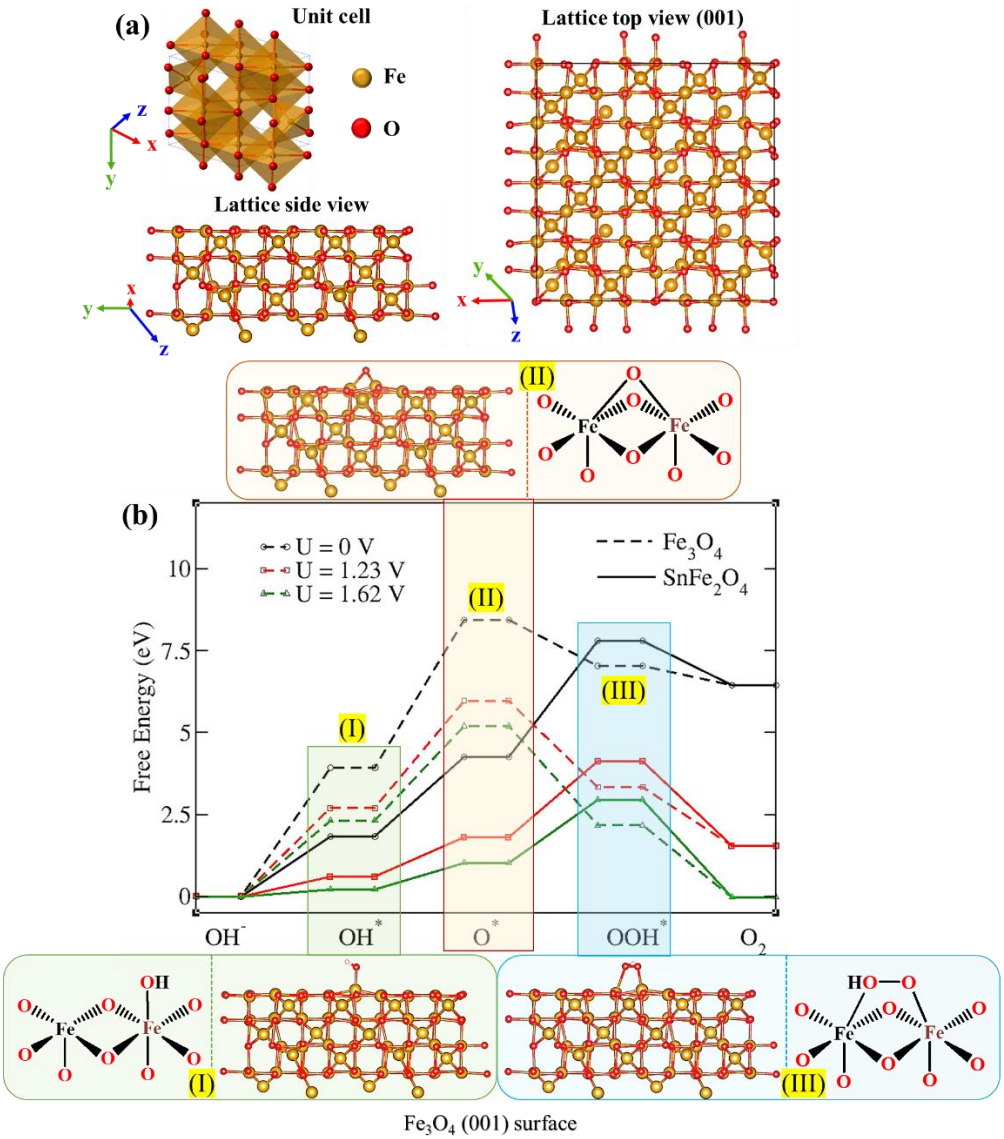

Figure S10. (a) A polyhedral unit cell of the Fe_3O_4 lattice and the 2 x 2 supercell of the Fe_3O_4 layer showing the top and side view of the lattice. (b) The free energy diagram of the OER of the Fe_3O_4 (dotted line) and on the (001) surface at potentials of U = 0 V (black line), 1.23 V (red line), and 1.62 V (green line) (vs RHE). The optimized OER intermediates on the Fe_3O_4 (001) surface shown in the inset.

Table 1. The free energy of the OER intermediates formed on the (001) plane of $SnFe_2O_4$ and Fe_3O_4 at potentials of U = 0 V, 1.23 V, and 1.62 V (vs. RHE).

OER Intermediate	Free energy (eV)@$SnFe_2O_4$ (001)			Free energy (eV)@Fe_3O_4 (001)		
	U = 0 V	U = 1.23 V	U = 1.62 V	U = 0 V	U = 1.23 V	U = 1.62 V
OH*	1.836	0.606	0.216	3.933	2.703	2.313
O*	4.265	1.805	1.025	8.438	5.978	5.198
OOH*	7.811	4.121	2.951	7.033	3.343	2.173
O_2	6.457	1.537	-0.022	6.457	1.537	-0.022

References.

1. P. Scherrer, *Math. Phys. Kl.* , 1918, **1918**, 98-100.
2. G. Kresse and J. Hafner, *Phys. Rev. B: Condens. Matter Mater. Phys.*, 1993, **47**, 558.
3. J. P. Perdew, K. Burke and M. Ernzerhof, *Phys. Rev. Lett.*, 1996, **77**, 3865.
4. S. Grimme, *J. Comput. Chem.*, 2006, **27**, 1787-1799.
5. H. J. Monkhorst and J. D. Pack, *Phys. Rev. B: Condens. Matter Mater. Phys.*, 1976, **13**, 5188.
6. S. Mondal, B. Mohanty, M. Nurhuda, S. Dalapati, R. Jana, M. Addicoat, A. Datta, B. K. Jena and A. Bhaumik, *ACS Catal.*, 2020, **10**, 5623-5630.
7. S. Halder, A. K. Pradhan, P. Sivasakthi, P. K. Samanta and C. Chakraborty, *Mater. Today Chem.*, 2023, **32**, 101649.